

**PAPER-BASED ION-SELECTIVE ORGANIC ELECTROCHEMICAL TRANSISTORS FOR THE
DETERMINATION OF POTASSIUM**

MASTER'S DEGREE THESIS



UNIVERSITAT ROVIRA i VIRGILI

Marc Clua Estivill

Supervised by Dr Pascal Blondeau and Dr Francisco J. Andrade

Master's degree in Nanoscience, Materials and Processes: Chemical Technology at the
Frontier

TARRAGONA 2020/2021

PAPER-BASED ION-SELECTIVE ORGANIC ELECTROCHEMICAL TRANSISTORS FOR THE DETERMINATION OF POTASSIUM

Marc Clua Estivill

Master's Degree in Nanoscience, Materials and Processes (2020-2021)

Supervisors: Dr Pascal Blondeau and Dr Francisco J. Andrade

Department of analytical chemistry and organic chemistry. Universitat Rovira i Virgili,
Campus Sescelades, Marcel·lí Domingo 1, Tarragona 43007, Spain.

ABSTRACT

This work is devoted to the development and optimization of thick-film ion-selective organic electrochemical transistors, using the determination of potassium as a model system. The sensor has been fabricated through a simple and low-cost process using paper as a substrate. A conducting polymer channel made of PEDOT:PSS was functionalized with an ion-selective membrane. Therefore, unlike conventional gate-sensitive systems, channel functionalization was evaluated. The analytical performance shows outstanding sensitivity, with values up to 2585 $\mu\text{A}/\text{dec}$, which is more than 20 times higher than the values reported up to date for similar systems. Moreover, the applicability of this sensor has been successfully tested in artificial serum. Calibration curves in the range from 3 mM to 6 mM K^+ show the great potential of these type of devices to become new platforms for decentralized ion-sensing.

1 INTRODUCTION

The detection and quantification of ions are part of the routine analysis in clinical laboratories (blood and urine analysis)^[1], environmental monitoring (water, soil, and air control)^[2], and quality control (industry, pharmacy, and food)^[3]. Most of these determinations are performed in centralized laboratories, where the samples need to be extracted, transported, treated, and analysed. This requires time, resources, skilled staff, and instrumentation that may represent an issue for applications requiring constant monitoring. For instance, the potassium level in patients with chronic kidney disease has to be monitored frequently in order to avoid cardiovascular problems^[4]. Therefore, there is an increasing demand for fast, economic, and simple to use ion-sensing devices for a wide range of applications.

In the past decades, electrochemical sensors have drawn attention due to their high sensitivity, selectivity, quick response, potential for miniaturization, and affordability^[5]. These characteristics as well as their simple operation have made electrochemical sensors ideal tools for the

decentralization of chemical analysis. Indeed, they can be adapted to monitor, detect and quantify analytes out of the lab in real samples without the use of complex and costly equipment^[6]. The success of the glucometer illustrates well this approach^[7].

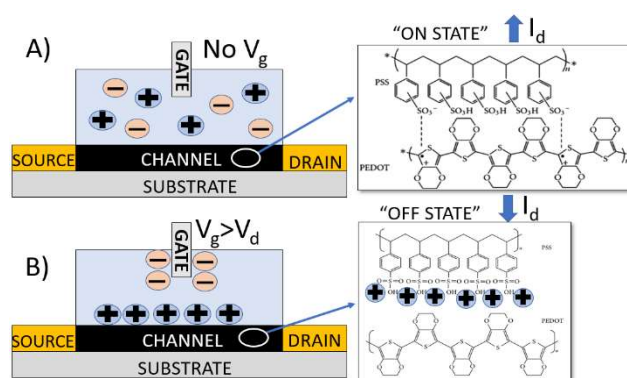


Figure 1: Schematic illustration of an OEET with PEDOT:PSS as the channel working in depletion mode. A) OEET on state after the application of a V_d where the PEDOT:PSS contains mobile holes allowing the current flow. B) OEET off state after the cation incorporation to the channel that reduces the number of holes and the current.

Organic electrochemical transistors (OEETs) are a new and promising group of electrochemical sensors that can be used for (bio)chemical sensing. Introduced more than 30 years ago by Wrighton

et al.^[8], OECTs are composed of three electrodes, i.e. the source, drain and gate, a conductive polymer (channel), and an electrolyte solution that provides mobile ions. The source and the drain are connected through the channel, which at the same time, is immersed into the electrolyte separately from the third electrode (gate). The working principle of these transistors is based on the variation of the electrical conductivity of the channel produced by the incorporation of cations from the electrolyte. To control this process, a difference of potential is applied between the source and the drain (V_d), generating an electric current across the channel (I_d) (Figure 1 A). Then, a more positive potential is applied to the gate (V_g) electrode. This forces the cations from the electrolyte to migrate into the channel. (Figure 1 B). Several conducting polymers have been studied for the construction of OECTs, however, poly(3,4-ethylenedioxythiophene (PEDOT) doped with polystyrene sulphonate (PSS), known as PEDOT:PSS, has stood out above the others because of its low toxicity, easy manipulation (aqueous ink), cost, and applicability in multiple substrates^[9]. The conductive polymer has an oxidized (PEDOT⁺) highly conductive form (Figure 1 A), and a reduced (PEDOT) non-conductive form that are in equilibrium (Figure 1 B). The conductivity of the PEDOT:PSS is based on the stabilization of the PEDOT⁺ form that is produced by the electrostatic interactions with the negative charges provided by the sulphonate groups of the PSS^[10]. The cations that are forced to migrate into the channel shield this stabilizing effect, promoting the shift from the conductive to the non-conductive form (depletion mode). As a result of this process, known as de-doping of the conductive polymer, the ions that interact with the channel change the redox state of the organic polymer modulating the device conductivity^[10] (Figure 1 B). From an analytical standpoint, a change in voltage in the gate (V_g) produces a change in the conductivity of the channel, which is registered as a change on the I_d . This is the essence of the transduction mechanism of the OECTs. Since the difference in conductivity between the oxidized and reduced form is extremely high, the system is very sensitive. The capacity of the changes in V_g to modulate the I_d is defined as the

transconductance (g_m) and represents the transistor most relevant parameter (1):

$$g_m = -\frac{\Delta I_d}{\Delta V_g} \quad (1)$$

Higher transconductance implies greater changes in the current after the application of a specific V_d ^[11], i.e., the transconductance is the sensitivity of the system to changes in V_g . This particular characteristic of OECTs has encouraged its implementation as sensors by functionalizing the gate or the channel with different strategies allowing the detection of analytes such as metabolites (glucose^[12] and lactate^[13]), ethanol^[14], humidity^[15], and pH^[16], among others.

Maximum transconductance is achieved when the voltage drop applied by the gate falls in the vicinity of the channel. This means that optimum results are obtained by minimizing the capacitance of the gate. A Ag/AgCl electrode, for example, is considered one of the ideal gates^[10]. For this reason, attempts to use an ion-selective electrode as a gate did not provide satisfactory results, since the phase-boundary potential drops on the surrounding of the ion-selective membrane^[17]. To overcome these issues, Malliaras *et al.* have recently reported an OECT to detect ions by integrating an ion-selective membrane (ISM) cast onto the channel^[18]. They hypothesized that the interaction between the ISM and the target ion originates a potential bias in the ISM surface that force the cations enter and de-dope the channel with a double capacitor layer originated at the interfaces (see Figure 3 A and section 3.1). With this approach, the detection of sodium with sensitivities of 50 $\mu\text{A}/\text{dec}$ in the $10^{-4} \text{ M} - 10^{-1} \text{ M}$ range with a limit of detection (LOD) of $1.5 \cdot 10^{-5} \text{ M}$ were achieved. Their work demonstrated the design of new OECTs where the transistor, for instance, is incorporated in a wearable patch to monitor, with high precision, NH_4^+ and Ca^{2+} in sweat during physical exercise^[19]. Latest reports suggested the integration of an internal ion reservoir intermediate layer between the ISM and the channel to improve the OECT sensitivity, since the number of cations that interact with the channel increases. This sensor model was successfully tested with PSS as a cation reservoir, and for the first time,

response for potassium ($98 \mu\text{A}/\text{dec}$) and sodium ($224 \mu\text{A}/\text{dec}$) was obtained in the $10^{-4} \text{ M} - 10^{-1} \text{ M}$ range^[20]. Despite these improvements, the processes employed to fabricate the OECTs requires complex techniques, such as spin coating, lift-off, and electron beam evaporation to control the channel geometry (thin-film channels of few nm) and the components deposition, increasing the cost per sensor.

For this reason, the objective of this report is to develop and optimize a new methodology to manufacture low-cost ion-selective organic electrochemical transistors (IS-OECT) for potassium sensing. In comparison with other works, the IS-OECT is fabricated using paper substrates and thick-film PEDOT:PSS channels technology recently developed in our labs, which will be functionalized with an ISM. The construction was optimized through different designs, including several channel composites, thickness, ISM modifications and electrical parameters, in order to maximize analytical performance parameters. Finally, to evaluate the sensor applicability and advantages with respect to other alternatives, tests for the determination of potassium in artificial serum were performed. The outstanding sensitivity and enhanced precision demonstrated by this system show promise as a future platform for decentralized measurements.

2 EXPERIMENTAL SECTION

2.1 MATERIALS AND METHODS

All chemicals used were purchased from Sigma – Aldrich (Darmstadt, Germany, EU). Channel construction: high conductivity grade poly(3,4-ethylenedioxythiophene) doped with polystyrene sulphonate (3-4 wt %) in an aqueous solution and Nafion® 117 solution (5 wt %) in a mixture of aliphatic alcohols and water were used. Ion-selective membrane: potassium ionophore I $\geq 95.0 \%$, potassium tetrakis(4-chlorophenyl) borate $\geq 98.0 \%$, 2-Nitrophenyl octyl ether (NPOE) $\geq 99.0 \%$, Poly(vinyl chloride) high molecular weight (PVC) and anhydrous tetrahydrofuran (THF) $\geq 99.9 \%$.

Analytical grade salts for the standard solutions of KCl, NaCl, NH_4Cl and LiCl and $\text{MgCl}_2(6\text{H}_2\text{O})$ for the background electrolyte solution were used. Artificial

serum preparation: NaCl (6.487 g/L), NaHCO_3 (2.436 g/L), K_2HPO_3 (0.383 g/L), $\text{MgCl}_2(6\text{H}_2\text{O})$ (0.162 g/L), urea (0.150 g/L) and glucose (0.847 g/L). The standards were diluted with the background electrolyte ($\text{MgCl}_2(6\text{H}_2\text{O})$ 0.1 M) to have a constant ionic strength after the standard addition. All remaining solutions were prepared using MilliQ water (MilliQ water systems, resistivity $18.2 \text{ M}\Omega/\text{cm}$ ($25 \text{ }^\circ\text{C}$), SYNERGY® UV SYSTEMS, Merck KGaA, Darmstadt, Germany).

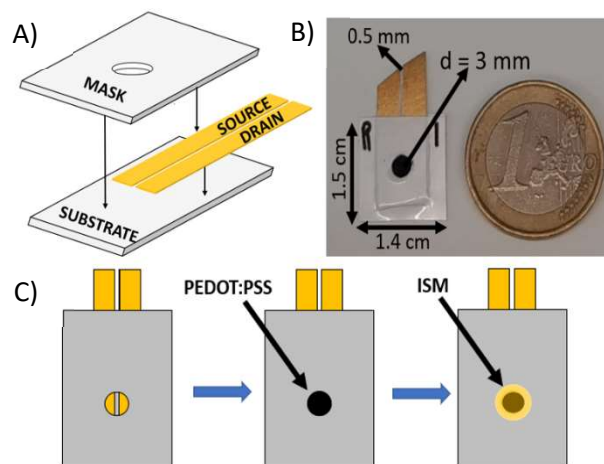


Figure 2: Illustration with the IS-OECT architecture. A) The source and the drain are covered by the paper mask and the substrate. B) Picture with the final sensor disposition and lengths. C) Channel and ISM coating in the exposed area.

2.2 IS-OECT FABRICATION K^+

OECT fabrication: The IS-OECT main structure is fabricated based on the last work published by the group^[21]. Briefly, a 100 nm gold layer is sputtered on top of a paper substrate to produce the source and the drain electrodes. An adhesive tape placed on the paper before the sputtering is then removed, producing a suitable gap between the two electrodes. A mask made with a water-resistant adhesive paper and having a small window (3 mm diameter) was used to block the source and the drain, leaving only a small part of the electrodes exposed. PEDOT:PSS is then dropped cast onto the window covering all the exposed region. The channel is baked for 20 min at $100 \text{ }^\circ\text{C}$ and is left cooled down to room temperature. Thereafter, the channel is conditioned by immersion for 2 hours in a 10^{-2} M KCl solution with constant stirring. Finally, the system was rinsed three times with distilled water for 5 minutes (Figure 2 A-B).

ISM preparation: Details of this procedure can be found elsewhere^[22,23,24]. The ISM mixture is composed of potassium ionophore I (0.5 wt %), potassium tetrakis(4-chlorophenyl) borate (2 wt %), PVC (32.8 wt %), NPOE (64.7 wt %) and THF (1 mL/100mg). The solution is mixed and then sonicated for 10 minutes. The ISM is stored in the fridge at 8 °C.

Channel functionalization: When the channel is dry, the ISM is dropped cast three times, each time with 5 μ L of solution over all the PEDOT:PSS channel surface. The coatings are added, waiting 5 minutes between depositions. Finally, the ISM is left to dry overnight (Figure 2 C).

2.3 DEVICE CHARACTERIZATION

The electrical characterization and analytical performance are studied using a 2x4 mm Ag/AgCl flat tip probe (Warner INSTRUMENTS, Holliston, MA, USA) as the gate electrode (input voltage), a Keithley 6514 Electrometer (Keithley Instruments, Cleveland, OH, USA) to measure the output current and a power supply (TENMA, Element14, Newark, New Jersey, US) for the application of the gate and drain voltages.

3 RESULTS AND DISCUSSIONS

3.1 CHANNEL

The initial approach was based on the design proposed by Malliaras *et al.*, where a PSS intermediate layer between the channel-ISM coatings was incorporated as an internal ion reservoir^[20]. The main idea of our work was to substitute the PSS ionomer with a less hydrophilic polymer (Nafion) in order to avoid leaching and improve the sensor performance. Nafion is a negatively charged ionomer and would work as an ion-exchange membrane for cations. The working principle of this approach is that upon the analyte addition, the interactions at the phase boundary of the ISM would generate a double capacitive layer in the aqueous solution/ISM and ISM/Nafion interfaces. The potential bias produced by the recognition of cations with the ionophore would force cations from the Nafion layer to move into the PEDOT:PSS, leading to de-doping (Figure 3 A). This approach did not produce reproducible experimental results. At a first glance, it could be

observed that the Nafion layer cracked with time allowing cations to not only interact with Nafion but also with PEDOT:PSS in a non-controlled fashion. Therefore, we proposed as an alternative to this layered structure to make the channel using a composite made of PEDOT:PSS and Nafion. In this way, the internal ion reservoir would be dispersed within the conductive polymer phase. The working principle of this new approach to make the channel is similar to the first one. However, while one capacitive layer is formed at the interface of the ISM-solution, a poly-dispersed capacitive layer will be formed between the Nafion and the PEDOT phase. This should provide advantages compared to the two capacitive layers formed with the previous strategy (Figure 3 B).

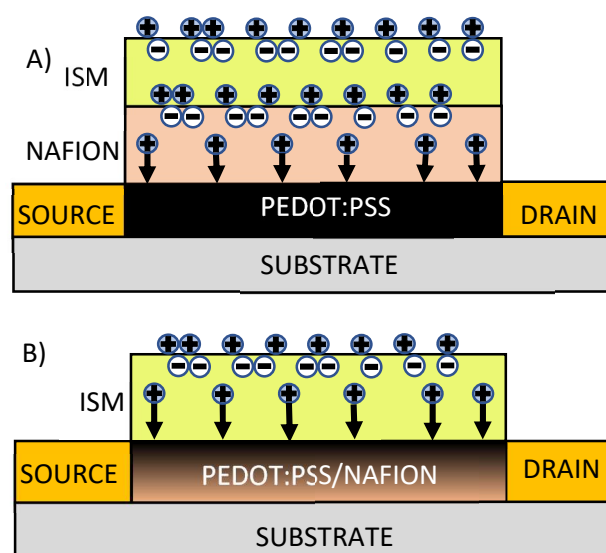


Figure 3: Illustration with the IS-OECT proposals and working methodology. A) Nafion intermediate layer approach. B) Channel composite with PEDOT:PSS and Nafion.

3.2 PEDOT:PSS/NAFION COMPOSITE

The use of the channel composite overcomes the issues of morphology previously observed. The system does not show cracks over time, the response is reproducible and therefore it appears as an effective alternative. In order to optimize this approach, different channel compositions were first prepared to assess the influence of the Nafion concentration on the analytical performance. As a starting point, the volume coated was 3 μ L to ensure the full window covering, and different PEDOT:PSS/Nafion compositions (%/%) of 25/75, 50/50, 75/25, 85/15, 95/5 and 100/0 were selected.

The initial experimental conditions were set at $V_g=0.75$ V and $V_d=-0.4$ V. In all these experiments, 0.1 M $MgCl_2$ was used as background electrolyte. Calibration curves for K^+ were performed in the 10^{-6} M - 10^{-1} M range. Remarkably, this approach showed in all cases good response for potassium. This means that the initial hypothesis, regarding an internally dispersed ion-reservoir, works as predicted. Table 1 summarizes the sensitivity and linear range for each composition. Maximum sensitivity is obtained with channels where the Nafion content was between 5-15 % and then drops as increase the Nafion %. As the Nafion concentration increases, less cations may reach the PEDOT:PSS layer thus, reducing the possibility that cations interact with the PEDOT:PSS to produce de-doping. In addition, as the PEDOT:PSS content decreases the current goes down and so does the capacity of the conducting polymer to be de-doped. This effect can be characterised by the channel static electrical resistance: as the Nafion concentration increases, the higher the channel resistance.

Table 1: Sensitivity and linear range for different channel compositions.

Nafion (%)	Sensitivity ($\mu A/decade$)	Linear range (M)
0	924	$10^{-3} - 10^{-1}$
5	1286	$10^{-3} - 10^{-1}$
15	1187	$10^{-3} - 10^{-1}$
25	732	$10^{-3} - 10^{-1}$
50	635	$10^{-3} - 10^{-1}$
75	67	$10^{-3} - 10^{-1}$

Modifying the channel geometry implies changes in the OECT transconductance and may therefore tune the sensor analytical performance. Bernards and Malliaras explained this effect following the models proposed for metal-oxide semiconductor field-effect transistors (MOSFET). They demonstrated that the OECT transconductance is related to the width (W), length (L) and thickness (T) of the channel (2)^[25].

$$g_m \propto \frac{W \cdot T}{L} \quad (2)$$

Hence, if the channel thickness increases, the transconductance is enhanced according to (2). However, these changes may affect other relevant parameters like the detection range because more cations are required to produce a detectable change

in the channel current, reducing the possibility to detect lower concentrations. The channel thickness can be controlled by the volume of composite used. For this reason, different volumes (5, 3, 2, 1.5 and 1 μL) were used to make channels, while keeping a constant composition (75 % PEDOT:PSS/25 % Nafion). The responses obtained are summarized in Table 2. Results show that the best sensitivity is achieved with volumes between 2 and 3 μL . Also, it can be observed that channels made with lower volumes allow improving the detection at lower ranges. For example, with the channel made with 1.5 μL composite the 10^{-5} M can be detected (Figure 4) and even 10^{-6} M for 1 μL channel. In general, better detectability at low concentrations is obtained with thinner channels. For this reason, the work was focused on these low volume channels that improve detectability. Also, the channel reproducibility needs to be considered because for a volume lower than 1.5 μL , the difficulty to manually spread the polymer through the entire window area increases. This reduces the channel reproducibility and therefore, the sensor applicability. For this reason, the final volume selected for the channel was 1.5 μL .

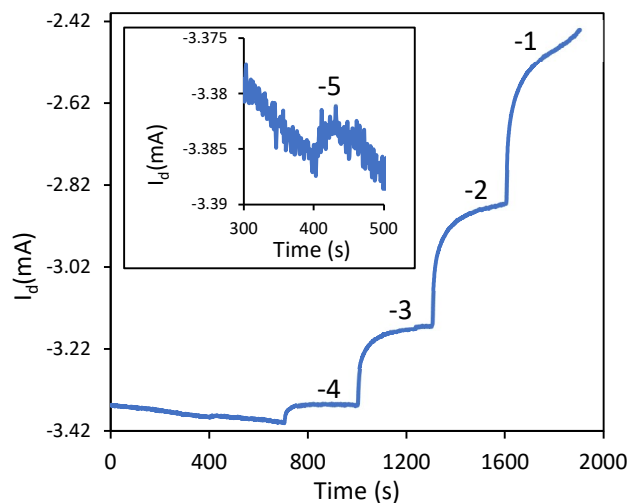


Figure 4: Time trace of a K^+ calibration curve using a 1.5 μL channel. Numbers indicate the negative logarithm of the concentration. The inset shows the -5 addition.

Table 2: Sensitivity and linear range results for the proposed channel volumes.

Channel Volume (μL)	Sensitivity ($\mu A/decade$)	Linear range (M)
5	595	$10^{-3} - 10^{-1}$
3	732	$10^{-3} - 10^{-1}$
2	1096	$10^{-3} - 10^{-1}$
1.5	357	$10^{-3} - 10^{-1}$
1	200	$10^{-3} - 10^{-1}$

With this new channel volume, experiments regarding the optimization of the composition amounts were repeated. Additionally, the instrumental conditions (V_g and V_d) were explored to optimize the sensitivity and linear range. While V_d was not significantly changed (-0.4 V), V_g was expanded to lower values (0.15 V). The results are shown in Table 3. In comparison with the higher volume channels (3 μ L), in these thinner channels, the effect of Nafion is more significant. For example, it is observed that the sensitivity is reduced at high concentrations. Noteworthy, the 50/50 and 25/75 composites are not included in the table due to the low stability and high resistance displayed by the sensor. Interestingly, one of the most remarkable difference is the excellent sensitivity observed for a channel made only of PEDOT:PSS. In general, as the Nafion concentration was decreased the sensitivity improved. It should be mentioned that the composite with 5 % Nafion shows a reduced sensitivity and issues with the sensor stability and reproducibility. We attributed this variation to problems forming stable and homogeneous composites. These results suggest that the addition of the ion reservoir leads to experimental problems and that the optimal channel composite is given with a 100 % PEDOT:PSS.

Table 3: Sensitivity and linear range for different 1.5 μ L channel composites.

Nafion (%)	Sensitivity (μ A/decade)	Linear range (M)
0	904	$10^{-5} - 10^{-1}$
5	254	$10^{-5} - 10^{-3}$
15	565	$10^{-4} - 10^{-2}$
25	357	$10^{-3} - 10^{-1}$

3.3 INSTRUMENTAL OPTIMIZATION

The gate and drain voltages affect the OECT operation modulating the electron current and the cation migration to the channel. Low gate voltages reduce the repulsion force that cations are exposed to but, high V_g may produce side reactions with other components from the electrolyte. The gate and drain voltages can be studied using the transfer curves where several V_g are applied in a constant V_d . In Figure 5 A, we can observe how the current (I_d) decreases as higher V_g are applied demonstrating the typical behaviour from OECTs in depletion mode. From this data, the transconductance can be

extracted following (1) and plot the g_m against the applied V_g (Figure 5 B). Here, the maximum transconductance is 1.30 mS for a $V_g=0.2$ V which are the typical values observed in OECTs^[10]. However, when the g_m is calculated using a sensor without the ISM changes are observed in the profile. The first one is the channel conductivity that is higher in sensors without the ISM. The second one is the g_m that increases to 8 mS at -0.1 V in the V_d and 0.1 V in the V_g . Therefore, the addition of the ISM reduced the OECT amplification characteristics. Parallely, calibration curves were performed with several V_g to obtain suitable applied voltages for the calibration curves. The selected V_g for the study is -0.15, 0 V, 0.15 V, 0.4 V and 0.75 V at a constant V_d (-0.4 V). At this point, we observe that not only the sensitivity is affected by the V_g but also the linear range and the selectivity (see 3.5.1). The best sensitivity is achieved when the V_g is 0 V (954 μ A/dec) and the lowest when the V_g reaches 0.4 V (247 μ A/dec).

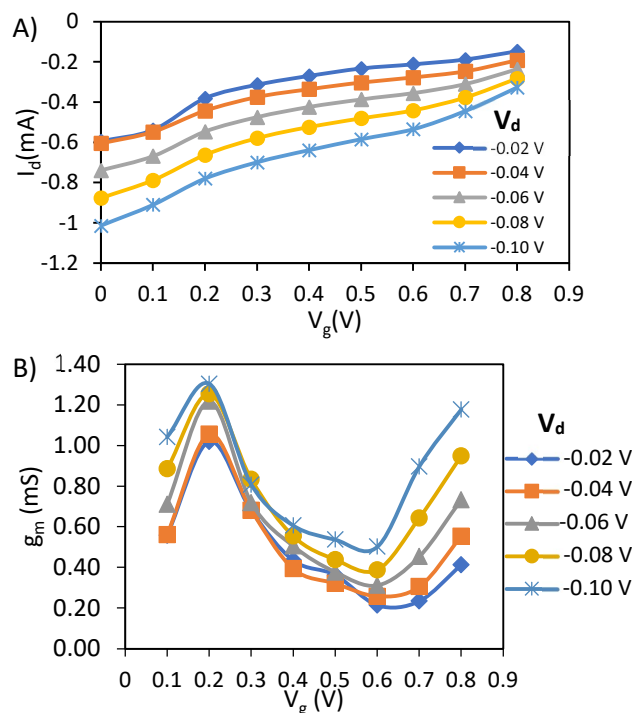


Figure 5: Electrical characterization using KCl 0.1 M as the electrolyte. A) Transfer curves for different V_d . B) Transconductance in front of the applied V_g .

3.4 ISM

The ISM is composed of an ionophore that selectively recognises the target ion, a cation-exchanger for the permselectivity, a polymeric matrix made with PVC and a plasticizer (NPOE) and THF. In potentiometry, the ISM volume may affect the sensor response^[23,24].

Therefore, 4 OECTs were made with membrane cast volumes of 5, 10, 15 and 20 μL (Figure 6 A). The results indicate that as the volume increases, sensitivity and linear range improve. This might be due to the increased difficulties to evenly spread the ISM along the entire area as the volume is reduced. The best performance is obtained at a membrane volume of 15 μL .

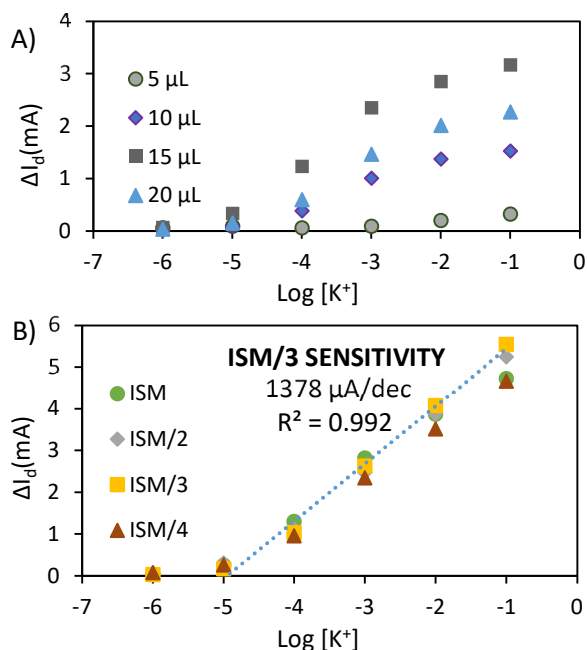


Figure 6: Baseline corrected results (I_0 -Iaddition) for the ISM optimization volume (A) and PVC/NPOE dilutions (B).

One additional factor to consider is the ISM thickness when reducing the load of polymer matrix (PVC and NPOE), while keeping the other components in the same proportion (ionophore and ion exchanger). Hence, experiments were performed where the polymer matrix was reduced to 50 % (ISM/2), 33 % (ISM/3) and 25 % (ISM/4) and is compared with the original ISM mixture (ISM) (Figure 6 B). The results show that the sensitivity increases with the reduction of the PVC and NPOE fraction until it reaches a point (ISM/4) where the sensitivity drops again. Several factors can be explaining this behaviour. First, reduced loading of the polymeric matrix will reduce the electrical permittivity of the membrane. This should increase the intensity of the electrical field produced inside the channel by the gate/membrane interface system. As a result, an enhanced transconductance is obtained as the membrane gets thinner. Moreover, previous studies suggest that the ion transport in ISM is reduced by the PVC membrane^[23]. Consequently, as we reduce the PVC

the ion transport may increase leading to the cations arrival to the channel increasing the sensitivity. It is also true that the lower the polymeric load, the weaker the mechanical resistance of the membrane. As less amount of PVC and NPOE is used, less resistant is the membrane and cracks appear in the window edges that limit the use of this latter composition.

In summary, the optimization leads to an OECT with a channel made of 1.5 μL cast of PEDOT:PSS with 15 μL cast of an ISM with 33 % of the polymeric matrix, measured at a $V_g=0$ V and $V_d=-0.4$ V.

3.5 ANALYTICAL PERFORMANCE

3.5.1 SELECTIVITY

Sensor selectivity depends on several factors, such as the ionophore recognition, cation exchanger permselectivity and ion hydrophobicity^[22]. Thus, depending on the ion properties and physical characteristics, different selective responses can be expected. Nonetheless, our results suggest that the working mode of the OECT provides a new way to control selectivity. Indeed, it has been found that the modification of the V_g can have an effect on the IS-OECT selective response. It should be pointed out that there is not yet a proper theoretical framework to deal with the selectivity of OECTs. Thus, in this work, the selectivity is calculated using the total response in the calibration curve (Final I_d (I_f) – Initial I_d (I_0)) rather than the selectivity coefficient. In essence, this selectivity coefficient would roughly measure how much the channel current will change upon the addition of a 10^{-1} M solution of an ion. In Figure 7 A, the total response for different ions at different V_g is presented for KCl, NaCl, NH_4Cl and LiCl calibration curves. At low V_g , the selectivity is comparable to the one observed in ion-selective electrodes. As it could be expected, ammonium interferes more than the other two salts because of its structural similarities with potassium. Conversely, Li^+ and Na^+ show the lowest response because their lipophilic properties disturb the cation-ion exchanger interaction. The best selectivity achieved is when the applied V_g is 0 V. Interestingly, at high V_g (0.75 V), the behaviour change and the selectivity is modified. The ion response is not affected by the ISM having similar

current differences between analytes. Therefore, at high V_g the system behaves like an unspecific cation exchange membrane. This behaviour can be attributed to the cation migration to the membrane, which overrides the selectivity provided by the ionophore. In other words, in this region the system is controlled by the strength of the electrical field provided by the gate. Although the selectivity is not good at high V_g , this particular characteristic may open an unexpected application for total ion content sensors substituting the ISM with a Nafion layer following previous works develop with potentiometric electrodes^[26,27].

3.5.2 REPRODUCIBILITY

For the reproducibility tests, 4 OECTs are independently fabricated the same day in the same conditions. Then, the OECTs are compared and tested with electrical (static resistance) and calibration procedures. First of all, the channel resistance is measured in all the sensor fabrication steps including, the annealing, the channel conditioning, and the ISM coating. In all OECTs resistance increases during the

fabrication process due to the cation incorporation to PEDOT:PSS. Besides, the resistance does not change significantly across the sensors. Once the OECTs were fabricated, the sensitivity and linear range were compared. The average sensitivity calculated is 1414 $\mu\text{A}/\text{dec}$ with a standard deviation of 52 μA for a $10^{-5} \text{ M} - 10^{-1} \text{ M}$ linear range proving sensor reproducibility. This result is more than 10 times higher than previous works developed with thin film IS-OECT (See Table 4).

3.5.3 DI WATER ELECTROLYTE

The electrolyte injects the ions into the channel. According to Bernards' model, this ion flow can be described as a resistor^[11]. Therefore, depending on the electrolyte used, the ion movement to the channel can be modulated, i.e. in more resistant solutions such as DI water, fewer ions will reach the channel. At this point, the electrolyte used for all the experiments were MgCl_2 to decrease this ion resistance and increase the ion flow. However, other works use DI water to ensure that the total response is only from the analyte and not also from the electrolyte. Thus, with the optimized sensor,

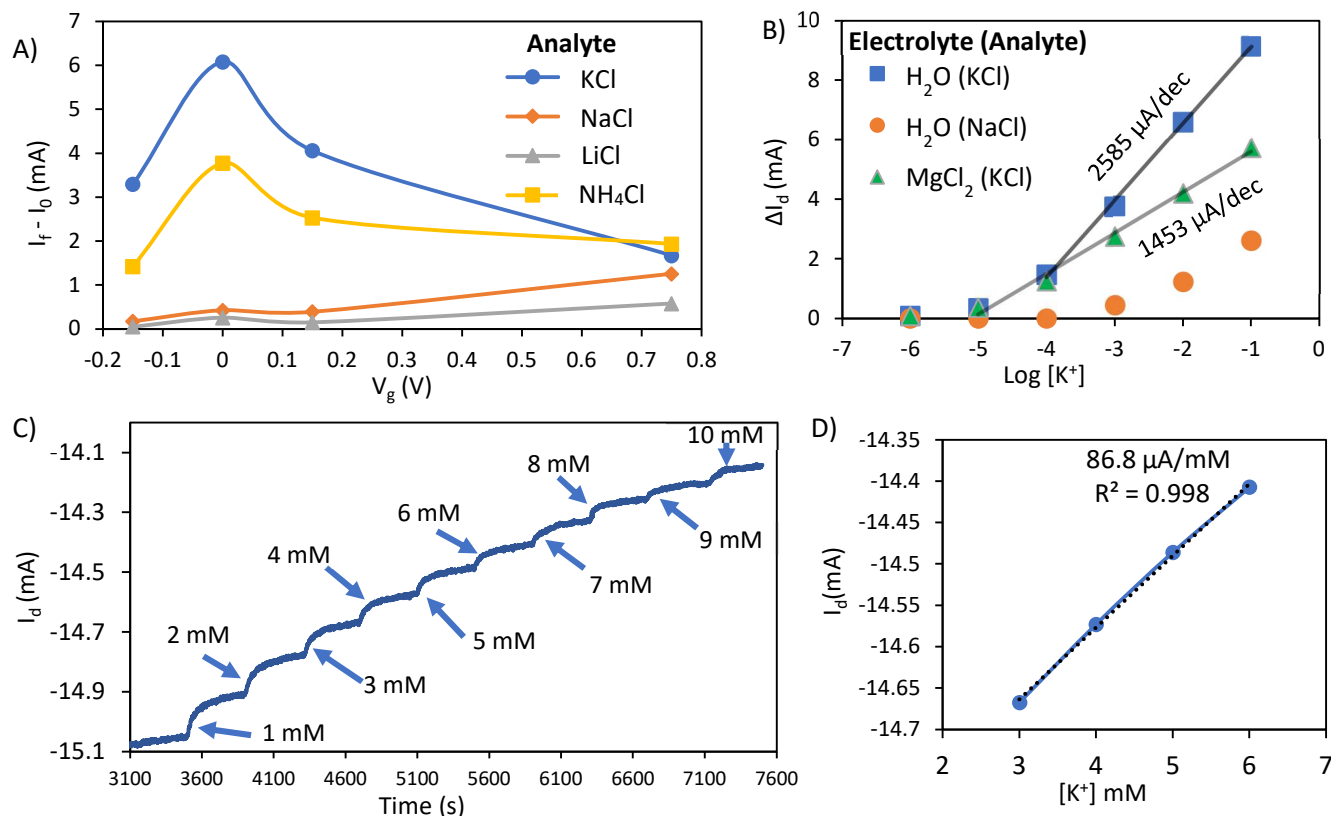


Figure 7: OECTs analytical performance results in a constant $V_d = -0.4$ V. A) Total sensor response ($I_f - I_0$) in different V_g for the target and interfering analytes. B) Baseline results for a KCl calibration curves in 2 separate electrolytes (DI H_2O and $\text{MgCl}_2(6\text{H}_2\text{O})$) using the same sensor at $V_g = 0$ V. C) Time trace with the 1 mM - 10 mM domain obtained in the precision test ($V_g = 0$ V). D) Calibration curve with the calculated sensitivity in the 3 mM - 6 mM linear range from the precision test in artificial serum.

calibration curves with the new electrolyte are performed for NaCl and KCl with the optimal conditions ($V_g=0$ V and $V_d=-0.4$ V). The sensitivity results are outstanding performing 20 times more sensitivity (2585 $\mu\text{A}/\text{dec}$) than previous works for a 10^{-4} M - 10^{-1} M linear range. Also, the sensor can still discriminate against the interfering ion (Figure 7 B).

3.5.4 PRECISION TEST

In order to demonstrate the sensor applicability, a precision test is performed using artificial serum as the electrolyte. In healthy patients, potassium levels in blood are normally between 3.5 mM and 5.5 mM. If these levels surpass the 5.5 mM (hyperkalemia) patient is at risk of having serious cardiovascular problems i.e., arrhythmia and heart attacks. On the other hand, if potassium levels are under 3.5 mM (hypokalemia) the patient feels constant muscle weakness and suffers, among others, diarrhoea and vomits. Hence, in patients with kidney diseases, it is very important to have constant potassium monitoring to avoid these problems^[4]. For this purpose, a calibration curve from 1 mM to 10 mM is carried out to test the sensor in a similar real-life sample (Figure 7 C). The sensor does not present significant noise or drifts in the baseline showing good stability in the sample matrix. The sensitivity is calculated for the typical target range used in medical assays showing a good precision (86.8 $\mu\text{A}/\text{mM}$) in the 3 mM - 6 mM domain (Figure 7 D). These values are adequate for decentralized clinical monitoring.

4 CONCLUSIONS

The optimization and test of a potassium IS-OECT have been presented in this work. The sensor design is based on a thick-film channel formed by PEDOT:PSS and an ISM with the plasticizer reduced (33 %). The results show an enhanced sensitivity in MgCl_2 (1453 $\mu\text{A}/\text{dec}$) and in DI water (2585 $\mu\text{A}/\text{dec}$) electrolytes that is more than one order of magnitude higher than previous works (Table 4). In addition, the linear range is comparable with paper-based ion-selective electrodes (10^{-5} M - 10^{-1} M) if MgCl_2 is used as the background electrolyte. These results are achieved following a simple and affordable paper-based sensor fabrication process, which do not require microfabrication techniques (i.e. photolithography) employed in other IS-OECT. The applied V_g provide a tunable sensor response that not only affects the sensor sensitivity but also the selectivity and linear range, expanding the OECT applicability. The sensor analytical performance gives excellent selectivities at low V_g and non-selectivity when high gate voltages are applied. Moreover, a test with artificial serum was performed in the 1 mM - 10 mM range providing good sensitivity and precision in the typical potassium levels in blood demonstrating sensor applicability in real-life samples.

Future experiments will be focused on sensor optimization by studying other parameters like the electrolyte. Besides, investigations regarding the physical behaviour of the sensor need to be done to demonstrate the sensor detection mode. Finally, the

Table 4: Summarize table with different ion-selective systems and their main fabrication methodologies and analytical performances.

Type of device	Ion	Sensitivity ($\mu\text{A}/\text{decade}$)	Sensitivity (mV/decade)	Fabrication process	Linear range (M)	Ref.
Paper ISE	K^+	-	58.1	Drop cast	$10^{-5} - 10^{-1}$	24
IS-EGOFET	Na^+	$\approx 0.25 - 0.5$	62	Soft molding process	$10^{-6} - 10^{-1}$	28
IS-OECT (Gel electrolyte)	K^+	≈ 47	48	Photolithography	$10^{-4} - 10^{-1}$	18
IS-OECT (PSS ion reservoir)	K^+, Na^+	98, 224	85	Photolithography	$10^{-4} - 10^{-1}$	29
Complementary amplifier OECT	K^+	-	2344	Photolithography	$10^{-5} - 10^{-1}$	30
Current driven OECT	K^+	-	414	Photolithography	$10^{-3} - 10^{-1}$	31
Paper IS-OECT	K^+	2585	-	Drop cast and sputtering	$10^{-4} - 10^{-1}$	This work

simple working model of the sensor could be used to fabricate a multiplex ion sensor using distinct channels and a single gate to expand sensor applicability.

5 ACKNOWLEDGMENTS

I would like to thank my supervisors Dr Francisco J. Andrade and Dr Pascal Blondeau, for their support, inspiration, and counselling during the development of this master thesis. Also, I would like to thank my partners Adil and Andres for their help and assistance in the laboratory. Finally, the URV for the opportunity to continue my professional formation with the award of the URV Master's grant for this course.

6 REFERENCES

- (1) Formica, D.; Schena, E. *Sensors*. **2021**, 21 (2), 1-5.
- (2) Hanrahan, G.; Patil, D. G.; Wang, J. *Journal of Environmental Monitoring*. The Royal Society of Chemistry. **2004**, 6 (8), 657–664.
- (3) Manikandan, V. S.; Adhikari, B. R.; Chen, A. *Analyst*. Royal Society of Chemistry. **2018**, 143 (19), 4537–4554.
- (4) Viera, J. A.; Wouk, N. *American Family Physician*. **2015**, 92 (6), 487–495.
- (5) Umasankar, Y.; Chen, S. M. *Sensors*. **2008**, 8 (1), 290–313.
- (6) Bakker E.; Telting-Diaz, M. *Anal. Chem.* **2002**, 74 (12), 2781–2800.
- (7) Adam Heller; Ben Feldman. *Chem. Rev.* **2008**, 108 (7), 2482–2505.
- (8) White, H. S.; Kittlesen, G. P.; Wrighton, M. S. *J. Am. Chem. Soc.* **1984**, 106 (18), 5375–5377.
- (9) Fan, J.; Rezaie, S. S.; Facchini-Rakovich, M.; Gudi, D.; Montemagno, C.; Gupta, M. *Org. Electron.* **2019**, 66, 148–155.
- (10) Rivnay, J.; Inal, S.; Salleo, A.; Owens, R. M.; Berggren, M.; Malliaras, G. G. *Nat. Rev. Mater.* **2018**, 3, 1-14.
- (11) Friedlein, J. T.; McLeod, R. R.; Rivnay, J. *Org. Electron.* **2018**, 63, 398–414.
- (12) Tang, H.; Yan, F.; Lin, P.; Xu, J.; Chan, H. L. W. *Adv. Funct. Mater.* **2011**, 21 (12), 2264–2272.
- (13) Currano, L. J.; Sage, F. C.; Hagedon, M.; Hamilton, L.; Patrone, J.; Gerasopoulos, K. *Sci. Rep.* **2018**, 8 (1), 1–11.
- (14) Bihar, E.; Deng, Y.; Miyake, T.; Saadaoui, M.; Malliaras, G. G.; Rolandi, M. *Sci. Rep.* **2016**, 6 (1), 1–6.
- (15) Nilsson, D.; Kugler, T.; Svensson, P. O.; Berggren, M. *Sensors Actuators, B Chem.* **2002**, 86 (2–3), 193–197.
- (16) Mariani, F.; Gualandi, I.; Tessarolo, M.; Fraboni, B.; Scavetta, E. *ACS Appl. Mater. Interfaces.* **2018**, 10 (26), 22474–22484.
- (17) Mousavi, Z.; Ekholm, A.; Bobacka, J.; Ivaska, A. *Electroanalysis.* **2009**, 21 (3–5), 472–479.
- (18) Sessolo, M.; Rivnay, J.; Bandiello, E.; Malliaras, G. G.; Bolink, H. J. *Adv. Mater.* **2014**, 26 (28), 4803–4807.
- (19) Keene, S. T.; Fogarty, D.; Cooke, R.; Casadevall, C. D.; Salleo, A.; Parlak, O. *Adv. Healthc. Mater.* **2019**, 8 (24), 1-8.
- (20) Han, S.; Yamamoto, S.; Polyravas, A. G.; Malliaras, G. G. *Adv. Mater.* **2020**, 32 (48), 1-8.
- (21) Ait Yazza, A.; Blondeau, P.; Andrade, F. J. *ACS Appl. Electron. Mater.* **2021**, 3 (4), 1886–1895.
- (22) Maksymiuk, K.; Stelmach, E.; Michalska, A. *Membranes (Basel)*. **2020**, 10 (10), 1–15.
- (23) Jackson, D. T.; Nelson, P. N. *J. Mol. Struct.* **2019**, 1182, 241–259.
- (24) Novell, M.; Parrilla, M.; Crespo, G. A.; Rius, F. X.; Andrade, F. J. *Anal. Chem.* **2012**, 84 (11), 4695–4702.
- (25) Bernardis, D. A.; Malliaras, G. G. *Adv. Funct. Mater.* **2007**, 17 (17), 3538–3544.
- (26) Grygolowicz-Pawlak, E.; Crespo, G. A.; Ghahraman Afshar, M.; Mistlberger, G.; Bakker, E. *Anal. Chem.* **2013**, 85 (13), 6208–6212.
- (27) Hoekstra, R.; Blondeau, P.; Andrade, F. J. *Electroanalysis.* **2018**, 30 (7), 1536–1544.
- (28) Schmoltner, K.; Kofler, J.; Klug, A.; List-Kratochvil, E. J. W. *Adv. Mater.* **2013**, 25 (47), 6895–6899.
- (29) Han, S.; Yamamoto, S.; Polyravas, A. G.; Malliaras, G. G. *Adv. Mater.* **2020**, 32 (48), 1–8.
- (30) Romele, P.; Gkoupidenis, P.; Koutsouras, D. A.; Lieberth, K.; Kovács-Vajna, Z. M.; Blom, P. W. M.; Torricelli, F. *Nat. Commun.* **2020**, 11 (1), 1–11.
- (31) Ghittorelli, M.; Lingstedt, L.; Romele, P.; Crăciun, N. I.; Kovács-Vajna, Z. M.; Blom, P. W. M.; Torricelli, F. *Nat. Commun.* **2018**, 9 (1), 1–10.